SOLID MATTER

ELECTRONIC STRUCTURE OF CHROMIUM- AND HYDROGEN-DOPED GaInN SOLID SOLUTIONS

S.V. SYROTYUK, V.M. SHVED

Lviv Polytechnic National University, Faculty of Semiconductor Electronics
(12, S. Bandera Str., Lviv 79000, Ukraine; e-mail: svsnpe@yahoo.com)

Electronic and magnetic properties of GaInN solid solutions doped with chromium and hydrogen impurities have been calculated with the use of the Green's function method. The obtained partial and total spin-polarized densities of states (DOS) point to a fundamental restructuring of the electronic structure in the crystals, which is induced by Cr substitutional and hydrogen interstitial impurity atoms. The changes are associated with the appearance of narrow hybridized states with s-, p-, and d-symmetries in the energy gap, which are absent from GaInN solid solutions.

1. Introduction

Diluted magnetic semiconductors draw attention of researchers because they can be used in spintronics, integrated optoelectronic devices, and quantum-mechanical nanostructures [1]. Indium-containing nitride alloys comprise an important component of opto-electronic devices. For instance, the active layer of short-wave light-emitting diodes and laser diodes is usually made up of $In_xGa_{1-x}N$ [2].

The energy of defect formation in AlN and GaN crystals, which is connected with doping the latter with donor (O, Si, Ge) and acceptor (Li, Be, Mg, Ca, Zn, Cd) impurities, were calculated in the framework of electron-density-functional theory (DFT) with the use of norm-conserving atomic *a priori* pseudo-potentials [3]. Hydrogens that appear in nitrides in the course of their growing following the MOCVD and HVPE technologies considerably affect their properties [3].

The increase of In content in the alloy provides, in principle, an opportunity to extend the range of light radiation emission from ultra-violet to red wavelengths. The GaN crystal with a 3% Cr impurity demonstrates

the largest value of magnetic moment [4]. However, In-GaN solid solutions doped with impurities of $3d$-elements have been little studied till now. The knowledge of the point defect origin in InGaN alloys is an important first step to understanding their role in physical processes. Modifications of the electronic structure in GaInN crystals under influence of the mutual action by Cr and H impurities are of both theoretical and practical values. Therefore, this work aimed at (i) calculating the partial and total electron densities of states in GaInN solid solutions, (ii) determining the magnetic moment of each atom in the lattice cell, (iii) calculating the total binding energies in solid solutions; and (iv) analyzing the variations in the electronic configuration of the crystal induced by Cr and H impurity atoms. In Section 2, the calculation method is described in brief. Section 3 is devoted to the analysis of the results obtained. Section 4 contains our conclusions.

2. Calculation Technique

Atomic and thermodynamic properties of semiconductors with defects are calculated with the help of atomic *a priori* pseudo-potentials [3, 5]. However, this method is rarely applied today to systems with impurities of d- and f-elements. Therefore, to calculate the electron structure of solid solutions with an impurity of a d-element, we used the software programs AkaiKKR [6]. The latter allows self-consistent calculations to be carried out for not only compounds with transition elements, but also disordered systems [7].

The program is based on the calculation of Green's function in the crystal [6],

$$G(\mathbf{r} + \mathbf{R}_n, \mathbf{r}' + R_{n'}; E) =$$

$$= -i\sqrt{E}\sum_{L} R_L^n(\mathbf{r}_<; E)H_L^n(\mathbf{r}_>; E)\delta_{nn'} +$$

$$+ \sum_{LL'} R_L^n(\mathbf{r}; E)G_{LL'}^{nn'}(E)R_{L'}^{n'}(\mathbf{r}'; E), \tag{1}$$

where $\mathbf{r}_<$ ($\mathbf{r}_>$) corresponds to either of two vectors, $\mathbf{r}$ or $\mathbf{r}'$, the length of which is smaller (larger). The wave functions $R_L^n(\mathbf{r}; E)$ and $H_L^n(\mathbf{r}; E)$ are given by the products of radial eigenfunctions and spherical harmonics,

$$R_L^n(\mathbf{r}; E) = R_L^n(r; E)Y_L(\mathbf{r}),$$

$$H_L^n(\mathbf{r}; E) = H_L^n(r; E)Y_L(\mathbf{r}). \tag{2}$$

Here, R is a regular solution of the radial Schrödinger equation in the central potential field $v^n(r)$. It is proportional to the Bessel spherical function $j_l(\sqrt{E}r)$ at the crystal site located in the muffin-tin (MT) sphere, i.e. provided that $r < R_{\mathrm{MT}}$. At the same time, H is an irregular solution, which describes the scattered wave beyond the MT-sphere and equals the Hankel spherical function $h_l(\sqrt{E}r)$. The latter does not exist at the point $r = 0$. Both H and R are single-site functions, whereas the structural matrix of Green's function $G_{LL'}^{nn'}(E)$ describes the relation between the solutions localized in different cells and, therefore, contains information on the scattering at various crystal sites.

The structural matrix of the unperturbed crystal, $G_{LL'}^{(0)\,nn'}(E)$, is determined by the Dyson equation

$$G_{LL'}^{(0)\,nn'}(E) =$$

$$= g_{LL'}^{nn'}(E) + \sum_{n''L''} g_{LL''}^{nn''}(E)\, t_{l''}^{n''}(E)G_{L''L'}^{(0)\,n''n'}(E), \tag{3}$$

where the matrix t_l^n for the potential $v^n(r)$ is defined according to the formula

$$t_l^n = \int\limits_0^{R_{\mathrm{MT}}} dr\, r^2 j_l(\sqrt{E}r)v^n(r)R_L^n(r; E), \tag{4}$$

and $g_{LL'}^{nn'}(E)$ is the free-electron Green's function. Now, the Green's function for a crystal with an impurity can be obtained from the modified Dyson equation,

$$G_{LL'}^{nn'}(E) = G_{LL'}^{(0)\,nn'}(E) +$$

$$+ \sum_{n''L''} G_{LL''}^{(0)\,nn''}(E)\Delta\, t_{l''}^{n''}G_{L''L'}^{n''n'}(E), \tag{5}$$

where $\Delta t_l^n = t_l^n - t_l^{(0)n}$ is the difference between the t-matrices for perturbed and perfect crystals.

In the KKR method, the self-consistent calculation of the electronic structure in a crystal with impurities is carried out according to the following procedure:

1) the initial potential of the crystal, $V_s^0(\mathbf{r})$, where s is the electron spin, is calculated;

2) the t-matrix for the unperturbed crystal, $t_{LL'}^{(0)}$, is calculated for both spin orientations;

3) the wave functions $R_L(\mathbf{r})$ and $H_L(\mathbf{r})$ are calculated and used to determine the matrix $t_{LL'}$ and the difference $\Delta t_{LL'}(E) = t_{LL'}(E) - t_{LL'}^{(0)}(E)$;

4) from Eq. (3), the matrix of structural constants of the unperturbed system, $G_{LL'}^{(0)\,nn'}(E)$, is obtained;

5) Dyson equation (5) is solved to determine the structural constants of the excited system, $G_{LL'}^{nn'}(E)$;

6) Green's function (1) is determined with the use of the obtained wave functions $R_L(\mathbf{r})$ and $H_L(\mathbf{r})$ and the matrix of structural constants $G_{LL'}^{nn'}(E)$;

7) the concentration of valence electrons is calculated by the formula

$$\rho_s^v(\mathbf{r}) = -\frac{1}{\pi}\mathrm{Im}\int\limits_{E_{\min}}^{E_{\mathrm{F}}} G_s(\mathbf{r}, \mathbf{r}; Z)dZ; \tag{6}$$

here, the integration is carried out in the complex plane from the valence band bottom $E_{\min}$ to the Fermi energy E_{F};

8) the wave functions of deep electrons and the corresponding electron concentration are determined;

9) the Poisson equation is used to calculate a corrected Coulomb potential of electrons in the crystal,

$$V_s(\mathbf{r}) = \int \frac{\rho_s(\mathbf{r}')}{|\mathbf{r} - \mathbf{r}'|}d\mathbf{r}'; \tag{7}$$

this potential is then taken as the initial one at the next iteration;

10) the total potential in the crystal is determined,

$$V(\mathbf{r}) = \sum_n \sum_i \sum_s v_s(\mathbf{r} - \boldsymbol{\tau}_i - \mathbf{R}_n), \tag{8}$$

here, the summation is carried out over the coordinates of crystal cells (n), the atoms in a cell (i), and the spin variables (s); in the course of calculations, the MT-potential approximation is used, and the disorder is taken into account in the framework of coherent-potential approximation (CPA);

11) the potential at a crystal site is determined as the sum $v(\mathbf{r}) = v_n(\mathbf{r}) + v_e(\mathbf{r}) + v_{xc}(\mathbf{r})$, where v_n is the Coulomb potential of the atomic nucleus, v_e the potential created by deep and valence electrons, and v_{xc} the exchange-correlation potential of all electrons;

12) in this work, the iterations were repeated until the convergence of for the total energy of the crystal with an accuracy of 10^{-8} Ry is attained; the required number of iterations was approximately equal to 100.

In our calculations, we used the exchange-correlation potential based on the local approximation for the spin density and taken in the parametrization presented in work [8]. Various parametrizations for the functionals of exchange and correlation energies are given in work [9]. The version selected by us (see work [8]) depends explicitly on the spin polarization parameter $\varsigma = (\rho_\uparrow - \rho_\downarrow)/\rho$, where $\rho = \rho_\uparrow + \rho_\downarrow$ is the total concentration of electrons, i.e. it is the sum of electron concentrations with different spin orientations. The value $\varsigma = 0$ corresponds to the paramagnetic state, and $\varsigma = 1$ to the ferromagnetic one. For the integration over the Brillouin zone, the Monkhorst–Pack method [10] with the $8 \times 8 \times 8$ mesh was used. The lattice constant in the GaInN solid solution with the sphalerite structure was calculated following Vegard's rule. Relativistic effects were taken into account in the scalar relativistic approximation with regard for the spin-orbit interaction, which allowed us to determine the spin and orbital magnetic moments for each atom in the elementary cell. The density of electron states for each spin orientation was calculated by the formula

$$n_s(E) = -1/\pi \mathrm{Im} \int d\mathbf{r} G_s(\mathbf{r}, \mathbf{r}, E), \qquad (9)$$

where G is the retarded Green's function [11]. The octahedral interstitial site (Vo) is localized at the point with the coordinates $(1/2, 1/2, 1/2)$ and the tetrahedral one (Vt) at the point with the coordinates $(3/4, 3/4, 3/4)$.

The calculations in the program were carried out in the framework of an all-electron self-consistent approach. The crystal potential was composed of the potentials of atomic nuclei on the basis of the wave functions of core and valence electrons.

3. Results and Their Discussion

In Table, the electronic and magnetic properties of GaInN solid solutions doped with chromium and hydrogen impurities are quoted. The following notations for solid solutions are used: A = $Ga_{0.72}Cr_{0.03}In_{0.25}N$, B = $Ga_{0.47}Cr_{0.03}In_{0.5}N$, and C = $Ga_{0.22}Cr_{0.03}In_{0.75}N$. The notations Vo and Vt stand for a hydrogen localized at an octahedral or tetrahedral, respectively, interstitial site.

The tabular data demonstrate that the magnitudes of spin magnetic moments located at hydrogen atoms are tens times as large as those centered at Ga, In, and N atoms. The dependence of these properties on the concentration of In atoms is also of interest. For instance, the magnitude of Fermi energy decreases with the growth of the In atomic fraction in the solution for both spin orientations. The spin-up electron density of states at the Fermi level steadily increases, whereas the corresponding variation for spin-down electrons is non-monotonous. The orbital magnetic moments exceed the spin ones only for nitrogen atoms, being smaller for all other atoms. In addition, the spin and orbital magnetic moments at other atoms are antiparallel, and the magnitude of spin moment considerably dominates. The values of μ_s and μ_L at Cr atoms are almost insensitive to a variation of the In concentration. The values of μ_s at H atoms located at interstitials Vo are the next, by magnitude, after the μ_s values at Cr atoms, being approximately five times as large as for H atoms located at interstitials Vt. It is of interest that μ_s at interstitials Vt are, on the contrary, also approximately five times as large as μ_s at Vo. At the same time, the values of orbital magnetic moment μ_L at interstitials Vo and Vt are of the same order of magnitude.

Note that even a minor difference between the data in the first and second rows of the table, i.e. between

T a b l e. Electron and magnetic properties of $Ga_{1-x-y}In_xCr_yN$ solid solutions with the hydrogen impurity (0.1%) located at the octahedral (Vo) or tetrahedral (Vt) interstitial site. Here, ε_F is the Fermi energy (eV), "up" ("dn") means the spin-up (spin-down) orientation, $n(\varepsilon_F)$ is the electron density of states at the Fermi level ($eV^{-1}cell^{-1}spin^{-1}$), and μ_s and μ_L are the spin and orbital, respectively, magnetic moments (μ_B)

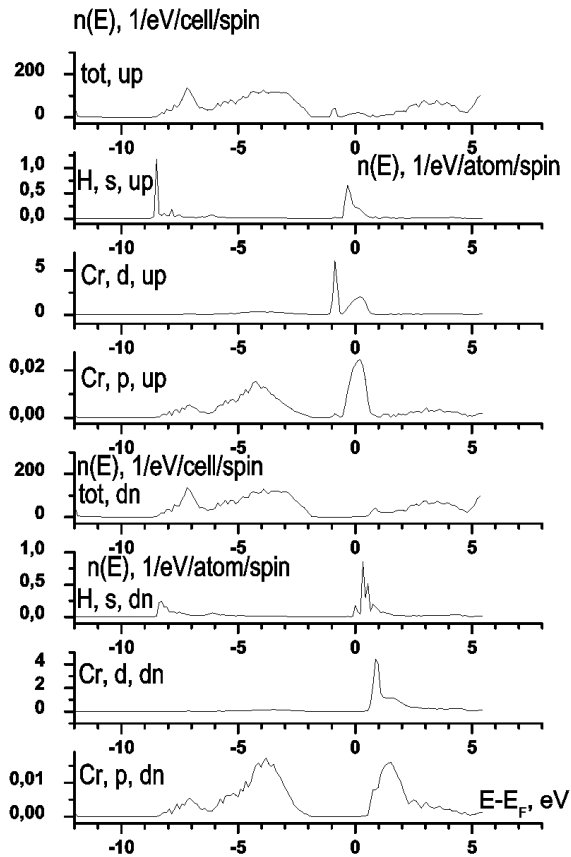|	A, Vo	A, Vt	B, Vo	B, Vt	C, Vo	C, Vt
ε_F, up	12.63583	12.61978	12.10218	12.09034	11.10843	11.09387
ε_F, dn	12.60426	12.58871	12.07691	12.06534	11.08384	11.06959
$n(\varepsilon_F)$, up	19.09036	18.95213	21.55657	21.39352	25.69298	25.83051
$n(\varepsilon_F)$, dn	2.08437	0.901478	2.228562	4.407322	1.001921	1.508838
μ_s on Ga	0.00262	0.00254	0.00236	0.00232	0.00269	0.00265
μ_L on Ga	–0.00008	–0.00008	–0.0001	–0.0001	–0.00006	–0.00006
μ_s on Cr	2.29948	2.28828	2.28881	2.28095	2.41515	2.40518
μ_L on Cr	–0.55957	–0.55982	–0.58629	–0.58582	–0.56397	–0.55473
μ_s on In	0.00195	0.00189	0.00154	0.0015	0.00132	0.0013
μ_L on In	–0.00026	–0.00026	–0.00021	–0.0002	0.00009	0.00009
μ_s on N	0.00147	0.00102	–0.00045	–0.00075	–0.00171	–0.00212
μ_L on N	0.00229	0.0023	0.00185	0.00186	0.00186	0.00184
μ_s on Vo	0.00108	0.00105	0.001	0.00099	0.00097	0.00096
μ_L on Vo	–0.00015	–0.00015	–0.00014	–0.00014	–0.00015	–0.00015
μ_s on H	0.29271	–0.06084	0.27598	–0.05717	0.26493	–0.07034
μ_L on H	–0.00045	–0.0001	–0.00044	–0.00007	–0.00045	–0.00006
μ_s on Vt	0.00589	0.00575	0.00488	0.00483	0.00436	0.00431
μ_L on Vt	–0.00009	–0.00009	–0.00006	–0.00006	–0.00006	–0.00006

Fig. 1. Partial and total electron densities of states in the $Ga_{0.72}Cr_{0.03}In_{0.25}N$ solid solution with the H impurity (0.1%) located at the interstitial site Vo

Fig. 2. The same as in Fig. 1, but for the H impurity (0.1%) located at the interstitial site Vt

the Fermi energies for opposite spin orientations, testifies to the existence of a non-zero magnetic moment in the crystal. Analyzing the data in the third and fourth rows of the table, we note that the substantial difference between the numerical values of electron density of states with opposite spins is a reliable indicator of the presence of a rather large magnetic moment in the crystal.

Now, let us proceed to the analysis of plots for the electron densities of states. In Figs. 1 to 6, the partial and total electron densities of states in $Ga_{1-x-y}In_xCr_yN$ solid solutions with an H impurity (0.1%) located at either Vo or Vt interstitial are depicted. The plots exhibit the partial p- and d-states of Cr atoms and the s-states of H ones as having the largest amplitudes, which is confirmed by the tabular data concerning the values of atomic magnetic moments in the solid solutions.

In Fig. 1, the partial and total electron densities of states in the GaInN solid solution with the Cr substitutional impurity are shown. Here, the impurity is located
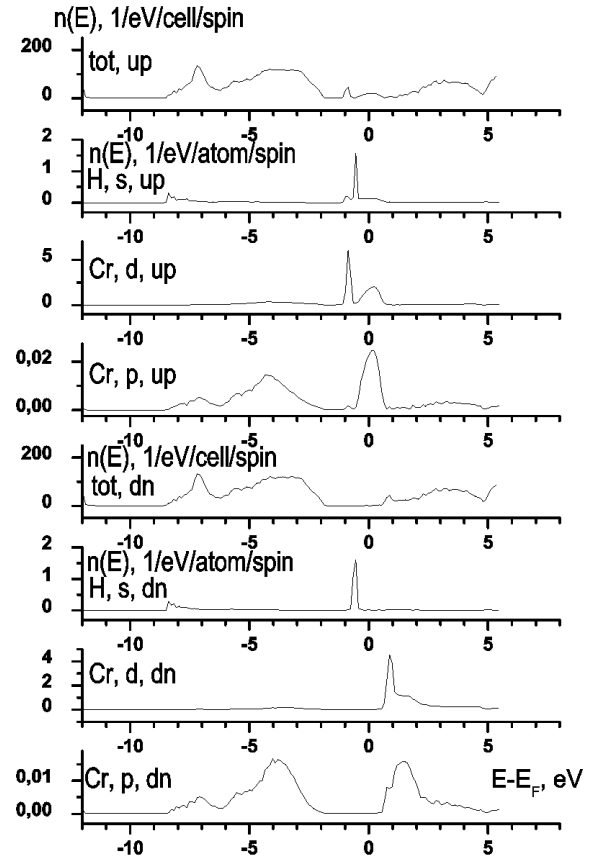
at the interstitial site Vo. The first four curves correspond to the spin-down orientation. The lowest three curves demonstrate that, in the energy gap, there emerge non-populated narrow bands of the p- and d-symmetry (they are associated with Cr atoms) and non-populated s-states of H atoms. The fourth curve corresponds to the total DOS. The next four curves correspond to the spin-up orientation. The fifth and sixth curves testify to the presence of narrow partially populated spin-up bands of the p- and d-symmetries in the energy gap, which originate from the Cr impurity. Note that these bands—both populated with electrons and free ones—are narrow and strongly hybridized. The seventh curve represents partially populated s-states of H. The eighth curve corresponds to the total DOS. It is evident that the total DOS underwent a modification in the energy gap induced by the influence of Cr and H impurities. Nevertheless, the structure of modified DOS can easily be explained, by using partial DOS.

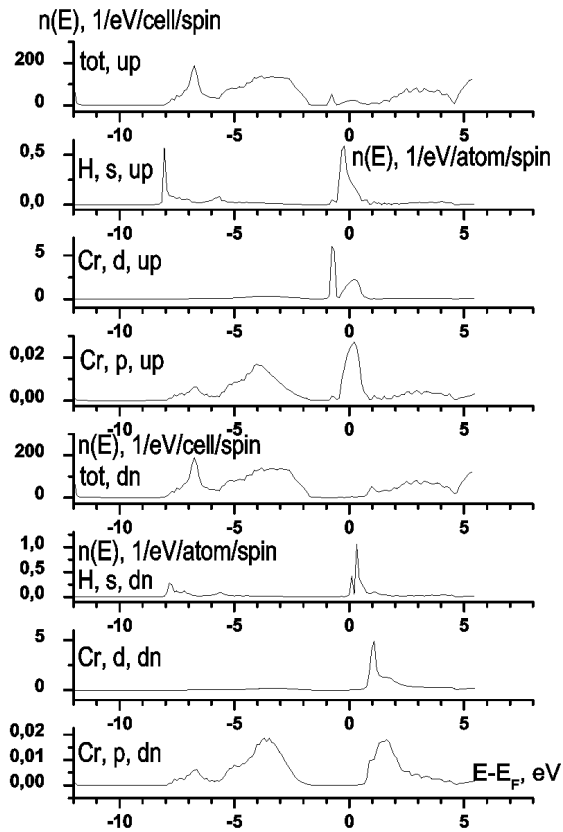In Fig. 2, the densities of states in GaInN crystals with Cr and H substitutional impurities are depicted. Here,

Fig. 3. Partial and total electron DOS in the $Ga_{0.47}Cr_{0.03}In_{0.5}N$ solid solution with the H impurity (0.1%) located at the interstitial site Vo

Fig. 4. The same as in Fig. 3, but for the H impurity (0.1%) located at the interstitial site Vt

the impurity atom is located at the interstitial site Vt. While comparing the partial DOS induced by Cr impurities and exhibited in Figs. 1 and 2, we see that they are almost identical. However, a detailed comparison between the curves that correspond to partial DOS at H atoms testifies to a considerable difference. In particular, in the case of hydrogen located at the interstitial site Vo, the narrow spin-down band is not populated; but if the hydrogen is located at Vt, the band concerned is populated. In the case of the hydrogen localization at the interstitial site Vo, the corresponding narrow spin-up band is only partially populated; however, this band is populated if H is located at the interstitial site Vt. Taking advantage of partial DOS at H atoms, which are shown in Figs. 1 and 2, we can qualitatively find that the magnetic moment is larger at the hydrogen atom located at an interstitial site Vo. Really, the value of magnetic moment is proportional to the difference between the areas under the curves corresponding to spin-up and spin-down orientations. This difference is larger for Fig. 1, being small for Fig. 2, and the corresponding
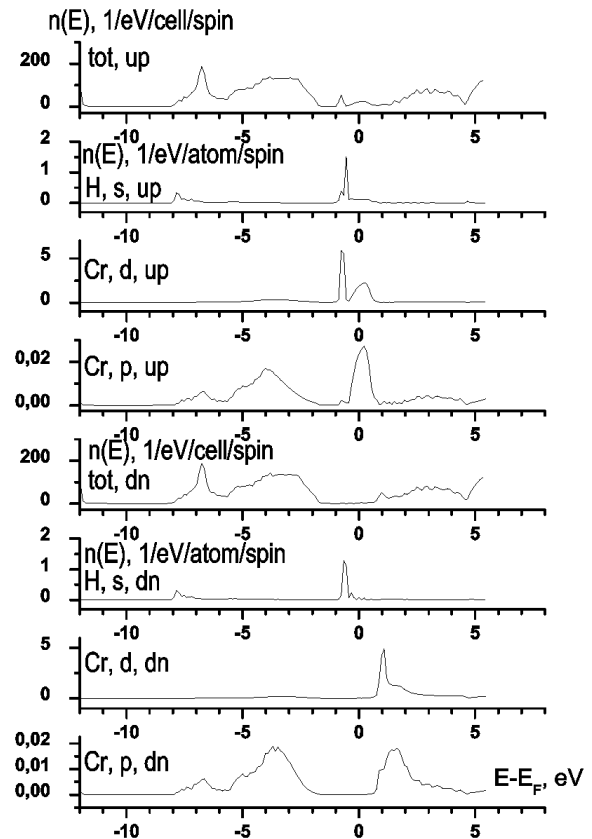
moments quoted in Table equal $0.29\mu_B$ and $-0.06\mu_B$, respectively.

In Figs. 3 and 4, the partial and total DOS are shown for the GaInN solid solution with the Cr substitutional impurity, in which the In content equals 50%, and the hydrogen impurity is located at the interstitial site Vo or Vt, respectively. From Fig. 3, one can see that the spin-down partial DOS at Cr and H atoms correspond to non-populated bands, whereas the spin-up partial DOS to partially populated ones. Figure 4 demonstrates that the spin-down and spin-up partial DOS at H atoms correspond to populated bands with the s-symmetry.

The curves in Figs. 5 and 6 exhibit the partial and total DOS in the GaInN solid solution with an In content of 75%. In Fig. 5, the partial spin-down DOS at Cr and H atoms correspond to non-populated narrow bands, and the spin-up DOS to partially populated ones. However, in Fig. 6, the partial DOS at H atoms correspond to the narrow populated spin-down band of the s-symmetry, and we have a partially populated
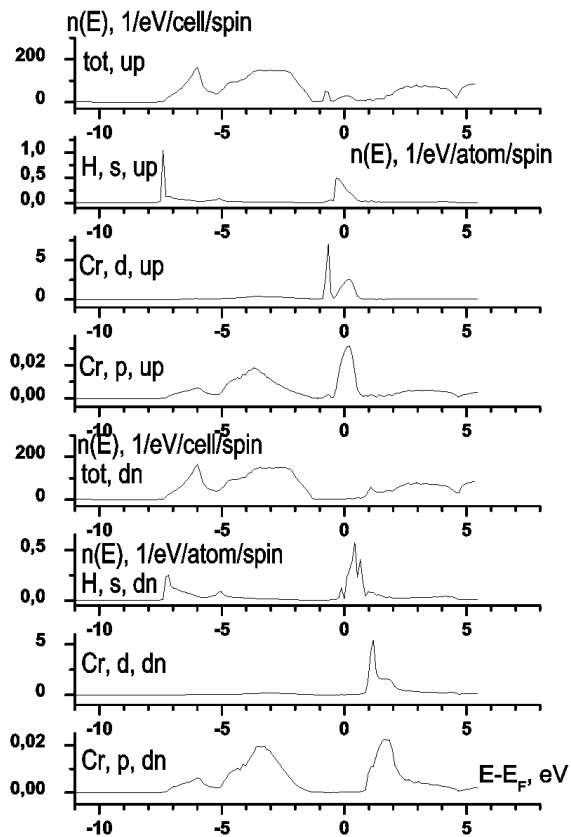
Fig. 5. Partial and total electron DOS in the $Ga_{0.22}Cr_{0.03}In_{0.75}N$ solid solution with the H impurity (0.1%) located at the interstitial site Vo

Fig. 6. The same as in Fig. 5, but for the H impurity (0.1%) located at the interstitial site Vt

band composed of s-states for the spin-up orientation. At the same time, the corresponding bands induced by hydrogen and represented in Figs. 2 and 4 are populated.

The presented results qualitatively agree with those obtained while *a priori* calculating the electron densities of states in the GaN crystal with the Mn impurity in the framework of the norm-conserving atomic pseudo-potential method [12]. In this method, the approximation of MT-potential is not used. From the results of work [12], one can see that the $3d$-states of manganese are located at the Fermi level, and the width of the impurity band approximately equals 1.5 eV. In works [13, 14], we can also find a qualitative comparison of the results obtained for GaN with the Mn impurity. It turned out that various *a priori* pseudo-potentials bring about $3d$-states of manganese that are also located at the Fermi level.

The authors of experimental work [15] revealed ferromagnetism in a GaN crystal with the Mn impurity and proposed a criterion, according to which this state
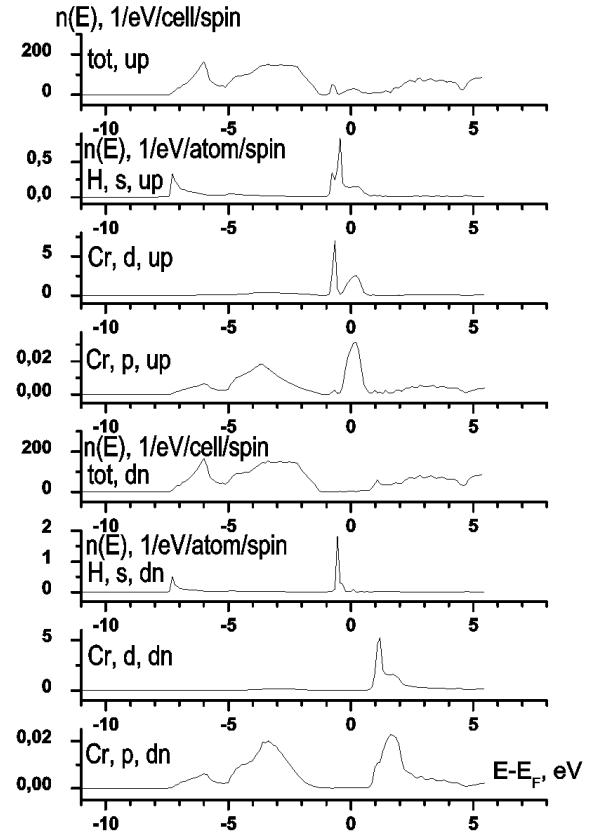
arises provided that the Fermi level is located in the band formed by Mn states that, in turn, are located in the energy gap of the matrix. In experimental work [16], ferromagnetism was found in a GaN crystal with the Cr impurity at room temperature, and a conclusion was drawn that GaN:Cr is a candidate for applications in spin electronics.

On the other hand, the available experimental data are often inconsistent. Some literature sources assert that ferromagnetism with a high T_C can be obtained in the GaMnN system [17]. The other sources consider antiferromagnetism [18] or paramagnetism [19] in GaMnN. The origin of magnetism in this system is also a matter of discussion [20]. Some researchers suppose that the observed ferromagnetic state can be associated with secondary phases, and GaMnN is a spin glass [21]. The others assert that no secondary phase is observed in single-crystalline GaMnN specimens with the ferromagnetic order [22].

We do not know about experimental and theoretical results for GaInN systems with impurities of transition $3d$-elements.

4. Conclusions

The partial and total DOS in GaInN solid solutions with the Cr substitutional impurity (3%) and hydrogen atoms (0.1%) in Vo or Vt interstitial sites have been calculated. The hydrogen impurity was found to have a considerable influence on the electron densities of states at the Fermi level for both spin orientations (see Table). The spin and orbital magnetic moments at atoms and interstitials were calculated. The orbital moment was obtained taking the spin-orbit coupling into account. The largest values of the spin and orbital moments were obtained for Cr atoms, and the largest spin moments for H atoms. The spin and orbital moments at all atoms in the solid solution weakly depend on the In content. Really, In and Ga are isovalent. However, the Fermi energies considerably decrease, as the In content increases, and the electron densities of spin-up states substantially grow.

Figures 1 to 6 brought us to a conclusion about an essential reconstruction of the electronic configuration in the GaInN solid solutions invoked by Cr and H impurities. In particular, the latter induce the appearance of s-, p-, and d-states of hydrogen and chromium in the energy gap.

Which interstitial site is the most probable for hydrogen atoms to be located at? Within the considered interval of the In content, the total binding energies in solid solutions calculated for H atoms located at either Vo or Vt interstitial sites are close by magnitude. In particular, the corresponding binding energies equal -5904.8713 and -5904.8711 Ry, respectively, if the In content equals 25%; -7872.4489 and -7872.4490 Ry, respectively, if the In content equals 50%; and -9840.1012 and -9840.1010 Ry, respectively, if the In content equals 75%. This means that the largest difference between the total binding energies equals 0.0002 Ry or 0.0027 eV. Hence, the localizations of hydrogen atoms at Vo or Vt interstitial atoms are almost equiprobable.

From Figs. 1 to 6, we may draw conclusion that the effective mass approximation is inapplicable in the narrow bands induced by chromium and hydrogen impurities.

1. K.S. Burch, D.D. Awschalom, and D.N. Basov, J. Magn. Magn. Mater. **320**, 3207 (2008).

2. H. Morkoc, *Handbook of Nitride Semiconductors and Devices, Vol. 2* (Wiley, Weinheim, 2008).

3. C.G. Van de Walle and J. Neugebauer, J. Appl. Phys. **95**, 3851 (2004).

4. N. Newman, S.Y. Wu, H.X. Liu, J. Medvedeva, L. Gu, R.K. Singh, Z.G. Yu, I.L. Krainsky, S. Krishnamurthy, D.J. Smith, A.J. Freeman, and M. van Schilfgaarde, Phys. Status Solidi A **203**, 2729 (2006).

5. C.G. Van de Walle and J. Neugebauer, Phys. Status Solidi B **248**, 19 (2011).

6. H. Akai, Phys. Rev. Lett. **81**, 3002 (1998).

7. N.H. Long and H. Akai, J. Phys. Condens.Matter **19**, 365232 (2007).

8. V.L. Moruzzi, J.F. Janak, and A.R. Williams, *Calculated Electronic Properties of Metals* (Pergamon, New York, 1978).

9. J.M. MacLaren, D.P. Glougherty, M.E. McHenry, and M.M. Donovan, Comp. Phys. Commun. **66**, 383 (1991).

10. H.J. Monkhorst and J.D. Pack, Phys. Rev. B**13**, 5188 (1976).

11. H. Ebert, *A Spin Polarized Relativistic Korringa–Kohn–Rostoker (SPR-KKR) Code for Calculating Solid State Properties* (Universität München, München, 2010); http://olymp.cup.uni-muenchen.de/ak/ebert/SPRKKR.

12. L. Kronik, M. Jain, and J.R. Chelikowsky, Phys. Rev. B **66**, 041203(R) (2002).

13. B. Sanyal, O. Bengone, and S. Mirbt, Phys. Rev. B **68**, 205210 (2003).

14. P. Mahadevan and A. Zunger, Appl. Phys. Lett. **85**, 2860 (2004).

15. E.A. Berkman, M.J. Reed, F..E. Arkun, N.A. El-Masry, J.M. Zavada, M.O. Luen, M.L. Reed, and S.M. Bedair, Mater. Res. Soc. Symp. Proc. **834**, J7.3.1 (2005).

16. J.H. Chun, and D.E. Kim, Phys. Status Solidi A **208**, 691 (2011).

17. S.-H. Wei and G.M. Dalpian, SPIE Proc. **6894**, 68940L (2008).

18. Y. Shon, Y.H. Kwon, Sh.U. Yuldashev, J.H. Lim, C.S. Park, D.J. Fu, H.J. Kim, T.W. Kang, and X.J. Fan, Appl. Phys. Lett. **81,** 1845 (2002).

19. K. Ando, Appl. Phys. Lett. **82**, 100 (2003).

20. Q. Wang, Q. Sun, P. Jena, and Y. Kawazoe, Phys. Rev. Lett. **93**, 155501 (2004).

21. S. Dhar, O. Brandt, and A. Tampert, Appl. Phys. Lett. **82**, 2077 (2003).

22. S.J. Pearton, C.R. Abernathy, G.T. Thaler, R.M. Frazieer, D.P. Norton, F. Ren, Y.D. Park, J.M. Zavada, I.A. Buyanova, W.M. Chen, and A.F. Hebard, J. Phys. Condens. Matter **16**, R209 (2004).

ЕЛЕКТРОННА СТРУКТУРА ТВЕРДИХ РОЗЧИНІВ GaInN
З ДОМІШКАМИ ХРОМУ І ВОДНЮ

С.В. Сиротюк, В.М. Швед

Р е з ю м е

Електронні та магнітні властивості твердих розчинів GaInN
з домішками хрому і водню були розраховані за мето-
дом функції Гріна. Отримані парціальні та повні спін-
поляризовані густини електронних станів вказують на доко-
рінну перебудову електронної структури кристала, спричинену
атомами заміщення Cr та міжвузловими домішковими атома-
ми водню. Зміни зв'язані з появою у забороненій зоні вузьких
гібридизованих зон s-,p- і d-симетрії, відсутніх у твердих роз-
чинах GaInN.